The Selection of Measurement Positions for BEM Based NAH Using a Non–conformal Hologram to Reduce the Reconstruction Error

Agustinus Oey† and Jeong-Guon Ih†

ABSTRACT

This paper explores the use of BEM based NAH to reconstruct the surface vibration of a plate in a rectangular finite cavity, in which the distances between sensors and the nearest points on the source surface are not equal. In such circumstances, different degree of information on propagating and non–propagating wave components will be detected by sensors at different positions, as well as the influence of measurement noise will vary significantly from the nearest points of measurement to the farthest ones. On the other hand, the condition number of the vibro–acoustic transfer function matrix relating normal surface velocities and field pressures will becomes high, numerically indicating an increase of linear dependency between rows of transfer function matrix. The combination of poor measurement and high condition number will result inaccurate reconstruction. Therefore, one approach to be investigated in this work is to select the measurement positions in such ways that reduce measurement redundancy, as it indicated by the condition number. The improvement is found to be significant in the numerical simulations utilizing two different criterions, spanning from over–determined to under–determined cases, and in the validation experiment.

Keywords: boundary element method (BEM), near–field acoustical holography (NAH), non–conformal hologram, ill–conditioning matrix, inverse problem, singular value decomposition (SVD).

1. Introduction

BEM based NAH is known to be very powerful in the source identification and visualization of many practical vibro–acoustic sources having irregular boundaries. Once the relation between source and field can be contained in what so called transfer function matrix, the reconstruction of surface vibro–acoustic parameters as backward problem and the prediction of field acoustic parameters, as forward problem, are carried out by means of matrix inversion. Due to the existence of measurement error and to the ill–posed nature of the transfer function matrix, the results obtained by inverse method are prone to inaccuracy.

The measurement error may come from noise given by the measurement system. And also, the conventional BEM based NAH inherited error from the hyper–singularity in the close near–field of the source surface as discussed in [1]. This problem can be alleviated with the use of nonsingular or weakly singular boundary integral formulation, proposed in [2]. Another factor to be taken into account is the sensor position mismatch that amplifies random error energy in the backward problem as concluded in [3].

In general, the measurement of field quantities must be recorded sufficiently close to the source surface so that the evanescent wave information falls within the dynamic range of the sensor [4]. Or, in other words, sensor located at far distance is less likely to contain information provided by the evanescent wave, which is very essential to achieve a good reconstruction result.

As studied in this paper, when a simple measurement plane, or hologram, is used in the measurement of sound quantity generated by sources having irregular shapes, the distance between sensors and their nearest points on source surface cannot be maintained same. Because the evanescent wave decay exponentially as it travel farther, the disparity in information on propagating and non–propagating wave components captured by sensors will contribute error.

It was found that the resulted transfer function matrix containing non–conformal measurements is more ill–posed than the one given by conformal hologram, and implies that non–conformal hologram involves a large number of non–unique field points. Therefore, the basic idea depicted in this work is to explore the use of field points selection to enhance reconstruction result.

In this paper, the effect of non–conformal hologram for different cases of distance variability was firstly described, and, followed by a brief discussion on simulation of field points selection using two different methods, as given later. Finally, a short report on an experiment was presented to confirm simulation.

2. A Brief Theory on BEM Based NAH

Based on the Kirchhoff–Helmholtz integral equation, the relation of the normal surface velocity $\{v_n\}_S$ and field pressure $\{p\}_f$ can be expressed in discrete form as [5],

$$\{v_n\}_S = [G]_v^{\ +}\{p\}_f \,, \qquad (1)$$

where, $[G]_v$ and $[\cdot]^+$ denote the transfer function matrix and the pseudo–inverse operator

† **Korea Advanced Institute of Science and Technology**
E-mail: oeyaugust@gmail.com, J.G.Ih@kaist.ac.kr
Tel: (042) 869-3075, Fax: (042) 869-8220

2.1. Inverse Formulation

By virtue of singular value decomposition (SVD), the normal surface velocity can be estimated as

$$\{\hat{v}_n\}_S = [W]_v [\Lambda^{-1}]_v [U]_v^H \{p\}_f \,, \quad (2)$$

where $[\Lambda]$ represents a diagonal matrix whose diagonal elements are non–zero singular values, while $[W]$ and $[U]$ are orthonormal matrices containing left and right singular vectors, respectively.

2.2. Regularization and Reconstruction Error

The solution given in Eq. (2) inherits ill–posed inverse problem due to a small cluster of singular values in transfer matrix $[G]_v$ that its inverse includes a strong amplification of very small signal components at higher frequencies and causes it to be very sensitive to noise and error. To resolve the problem, regularization techniques have been developed to suppress error amplification to an acceptable level and refine the reconstructed image [as example, 6–8]. However, these techniques were not employed here to emphasize the refinement given by selection of field points.

If the measurement noise $\{n\}$ coexists with the true signal and it is assumed as uncorrelated Gaussian random having zero mean and variance σ^2, the expected squared value of reconstruction error is given by,

$$E\left[\left(\{\hat{v}_n\}_S - \{v_n\}_S\right)^H \left(\{\hat{v}_n\}_S - \{v_n\}_S\right)\right] = \sigma^2 tr\left[[G]_v{}^H [G]_v\right]^{-1} \equiv \sigma^2 S_F \quad (3)$$

where S_F denotes the singularity factor that indicates the degree of singularity of $[G]_v$.

2.3. Optimal Selection of Field Points

Given in Eq. (3), reconstruction error is in proportion to the measurement noise variance and the singularity factor of the transfer function matrix. Choices of field points will greatly affecting singularity factor – or by other means, condition number – because the geometrical information of field points is one 'big' factor in the calculation of transfer function matrix. Therefore, field points need to be arranged in a way that provides a low singularity factor.

The simplest method is to combine a number of field points to result a small condition number. First, generate *m* field point candidates, and calculate all possible *m* transfer function matrices relating *n* source points to (*m*–1) field points. Then, take the average of condition numbers over the frequency range of interest, and select any combination that has the smallest average. Repeat this procedure *p* times to select (*m*–*p*) field points. In a similar way, the composite condition number technique, as proposed in [9], can be used to reduce computation time.

Alternatively, the effective independence (EfI) method selects field points that make the mode shapes of interest linearly independent. The contribution of *m* field points, as given in [6], can be determined by,

$$E_f = diag\left([U]_v [U]_v{}^H\right) \quad (4)$$

Then iteratively, (*m*–*n*) field points related to the smallest contribution value can be omitted one by one.

3. Simulation and Experiment Setup

A simple parallelepiped box having the dimensions of 0.5 m (w) x 0.5 m (h) x 1.5 m (l) was constructed to test an interior problem. Except the vibrating plate clamped at one end of the box, all walls were assumed rigid. The plate was made by 1 mm–thick steel sheet with size of 0.5 m x 0.5 m and was excited by an electro–dynamic shaker (B&K4809) at a point near the corner. Force transducer (Endevco 2312) and accelerometers (PCB 353B16) were used to measure excitation force and normal surface velocities at 49 evenly spaced points over the vibrating plane, respectively.

The boundary element model of parallelepiped box, as shown in figure 1(a), comprised of 726 linear triangular elements and 365 nodes having the characteristic length of 0.143 m. The plate was defined at a side that has different element distribution, at x = 0.00 m. Based on $\lambda/6$–criterion, the high frequency limit of interest was 400 Hz.

For the simulation, 30 different sets of field data were prepared. Every set contains 49 field points that randomly scrambled using normal distribution function for several mean value μ and variance σ^2. Figure 1(b) illustrates one arrangement, from which it can be inferred that variance is a measure of hologram conformality. In addition, 4 sets of 98 field point candidates were generated at a single mean value and almost equal variances, which were used in the simulation of field points selection.

In the experiment, realizing a hologram to contain any sets of data used in the simulation is difficult. Without loss of the nature of the problem, leaning hologram was chosen to imitate the diversity of source–field distances along the ***x***–direction. The minimum distance was chosen as 0.03 m, which is larger than one–fifth of the element characteristic length, thus avoids the hyper–singularity problem in the close near–field [2].

The test was conducted for two cases representing a different degree of distance inequality. Field pressures were measured at 49 evenly distributed positions using ¼–inch microphones (B&K 4935). In the first case (case 1, 9°), the maximum distance was 0.09 m, while for the second one (case 2, 18°) 0.18 m. For a comparison purpose, the field pressures on the flat hologram at 0.03 m was measured in a similar manner. Figure 1(c, d) displays the arrangement of leaning and flat holograms.

4. Data Analysis and Discussion

Using the first kind of field point data sets, 30 transfer function matrices, defined in Eq. (2), were calculated. The singularity factors and condition numbers of the matrices were plotted in figure 2.

The singularity factors increase exponentially with the growth of distance. Clearly, one can expect that the black solid lines, which belong to the flat holograms, have to be spaced equally in a log scaled graph. The other lines given by random holograms sharing a same mean value should stay within the neighbourhood of their corresponding black line. And as variance become small, the singularity factors of the random holograms will converge to the one given by the flat hologram. The trends are also true for the plots of the condition numbers, and it agree with the fact that field point located far from source and does not follow the curvature of source will cause high singularity.

The condition numbers grow rapidly to a large value at cavity resonance frequencies, which were 114 Hz, 228 Hz, and 343 Hz. At these frequencies, standing waves dominate the field and conceal any instantaneous quantities radiated by the vibrating plate. Therefore, the values detected by the sensors do not contain enough information to describe the source characteristic. It is an example of condition number increment originated from incomplete measurements.

4.1. Enhancement by the Selection of Field Points

By considering condition number and EfI value, the 98 candidates provided in the second kind of random data sets were removed one by one until it reach 35 points. In the process, the average reconstruction error of synthetic source normal velocities and noisy field pressures were calculated using two different measures, as follow,

$$e = \left\| \{v_n\}_S - \{\tilde{v}_n\}_S \right\|_2 \Big/ \left\| \{v_n\}_S \right\|_2 \times 100\,(\%) \tag{5}$$

and

$$MAC = \left| \{v_n\}_S^{\,T} \{\tilde{v}_n\}_S \right|^2 \Big/ \left| \{v_n\}_S \right| \left| \{\tilde{v}_n\}_S \right| . \tag{6}$$

MAC was used to assess the modal correlation between the actual and the reconstructed normal surface velocities.

Figure 3 displays the progress of condition number and measurement error. The error given at 158 Hz is lower than at 97 Hz due to the fact that the non–radiating higher modes are more strongly excited than the low frequency excitation, which is also the reason of small singularity factor at high frequency excitation.

In term of condition number, the EfI method ends with a higher number compare to its counterpart. However, the resulted reconstruction errors were relatively similar. It was also found that the removed field points were not always the one located at far and were varied with frequency. It is because the box adopted as interior case introduces a highly reactive field.

4.2. Experiment Validation

The field pressures images captured from the leaning hologram have relatively flat phase information at the side associated with measurements at far, compared to images given by flat hologram. As result, the reconstructed image has a somewhat degraded shape of modal mode, as can be observed in example visualized in figure 4(b) and (c).

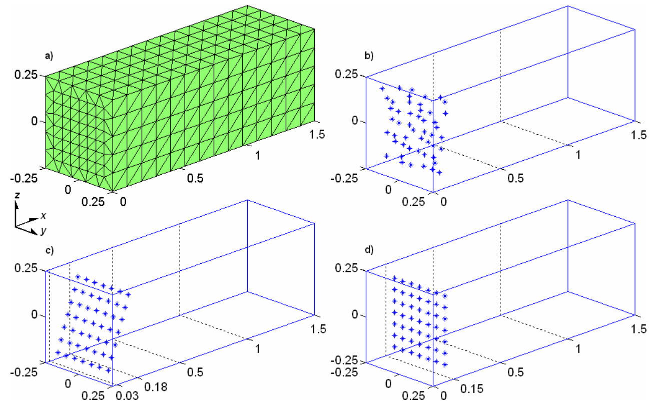

Figure 1. A view of (a) BEM model of a simple parallelepiped box, the arrangement of field points over (b) random hologram, (c) leaning hologram, and (d) flat hologram)

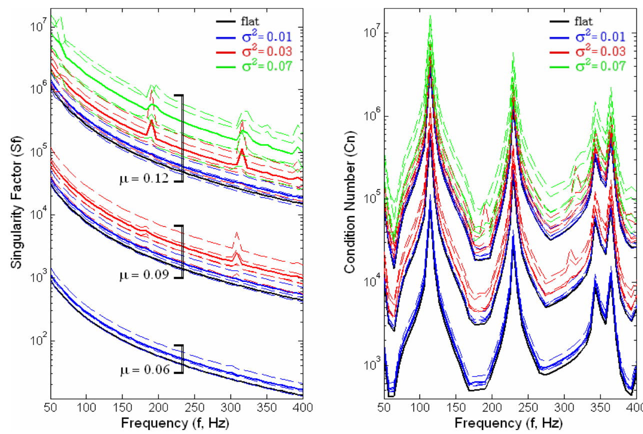

Figure 2. The singularity factors and condition numbers given by transfer function matrices calculated from 30 sets of field data.

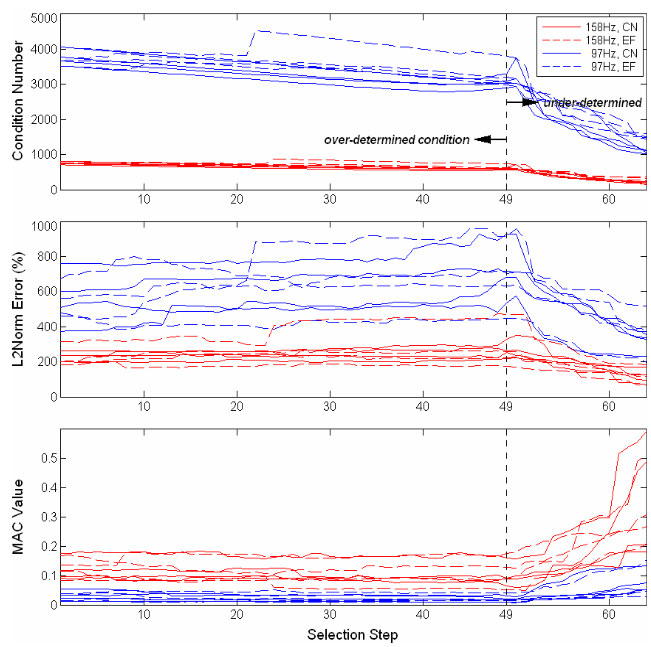

Figure 3. The evolution of condition number, reconstruction error, and MAC value with the removal of one field point a time.

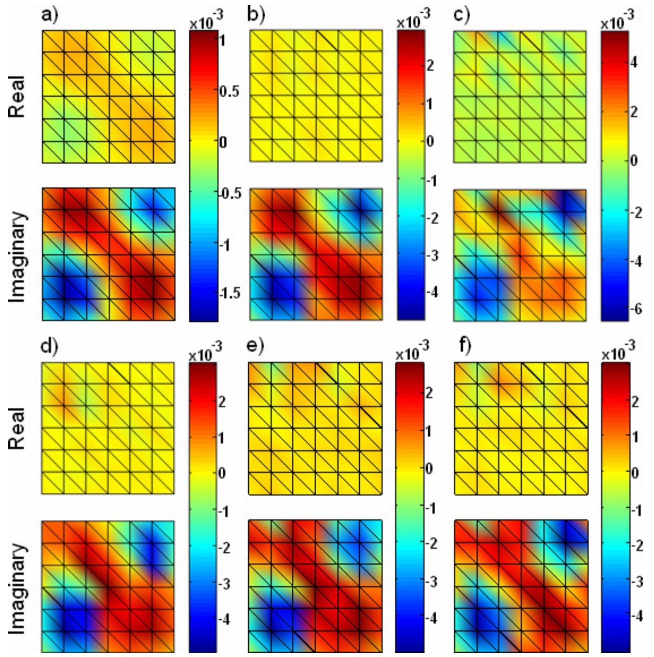

Figure 4. The images of normal surface velocity at 97Hz given by (a) the measurement on vibrating plate, the reconstruction of field data taken at (b) flat hologram and leaning 9^0 holograms having (c) 49 field points, 35 field points as resulted from the selection based on the (d) distance, (e) condition number, and (f) EfI value.

Based on the fact that the measurements at far contain little information given by the evanescent waves and signal to noise ratio is small, then one way worth to be tried in the experiment was to remove a number of field points at far. After removing out 14 field points at farthest distance, the reconstruction result was found to be better than the initial arrangement. Figure 4(d) shows one example at 97 Hz.

Distance is obviously one factor, however, because of the irregularity of source shape, the sound field become so much complex so that wave front does not always follows the source shape. It means that the field points selection based on distance only cannot be regarded true for all cases. Accordingly, the methods based on the condition number and EfI value, described in section 2.3, can offer a better way in arranging field points.

Table 1 summarized the experiment outcomes at 97 Hz and 158 Hz, and confirms the simulation finding, i.e. good reconstruction result can be expected by arranging field points to produce small singularity. The results given by the methods based on condition number and EfI are better than by discharging out the measurement point at far, especially for the leaning 18° hologram. Many of the removed field points were located at nodal points and at far.

One interesting phenomenon observed in simulation and experiment was that when the problem was drawn to an under–determined case, the reconstruction error becomes small. It is due to the transfer function matrix that has a very large condition number so the problem is effectively under–determined even tough the number of field points is larger than the number of source points.

Table 1. Reconstruction error and MAC value given by the flat hologram and leaning holograms: before (49pts) and after (35pts) the removal of 14 field points.

Freq. (Hz)	Reconstruction Error (%)						MAC Value					
	49 points			35 points, Leaning			49 points			35 points, Leaning		
	Flat	Leaning		Dist.	CN	EFI	Flat	Leaning		Dist.	CN	EFI
97	26	9^0	32	27	27	28	0.97	9^0	0.63	0.86	0.84	0.80
158	29		47	31	31	32	0.84		0.36	0.73	0.76	0.76
97	26	18^0	2200	91	76	76	0.97	18^0	0.00	0.08	0.11	0.12
158	29		1200	115	39	83	0.84		0.00	0.05	0.54	0.08

5. Conclusion

A selection of field points to enhance reconstruction result of BEM based NAH using non–conformal hologram has been presented, revealing a sense of 'regularization' by discharging measurement points that contribute singularity. On average, the reconstruction improvement owing to the selection of field points methods was about 60%, which is considerably a significant result.

Acknowledgement

This work was partially supported by Korea Research Fund (KRF) and BrainKorea(BK)21 Project.

References

[1]. B.-U. Koo, B.-C. Lee, J.-G. Ih, "A non–singular boundary integral equation for acoustic problems", *J. Sound Vib.* **192**, 263-279 (1996).

[2]. S.-C. Kang, J.-G. Ih, "Use of non–singular boundary integral formulation for reducing errors due to near–field measurements in the boundary element method based near–field acoustic holography", *J. Acoust. Soc. Am.* **109**, 1320-1328 (2001).

[3]. K.-U. Nam, Y.-H. Kim, "Errors due to sensor and position mismatch in planar acoustic holography", *J. Acoust. Soc. Am.* **106**, 1655-1665 (1999).

[4]. E. G. Williams, J. D. Maynard, "Holographic imaging without the wavelength resolution limit", *Physical Review Letters* **45**, 554-557 (1980).

[5]. B.-K. Kim, J.-G. Ih, "On the reconstruction of the vibro-acoustic field over the surface enclosing an interior space using the boundary element method", *J. Acoust. Soc. Am.* **100**, 3003-3016 (1996).

[6]. B.-K. Kim, J.-G. Ih, "Design of an optimal wave-vector filter for enhancing the resolution of reconstructed source field by near-field acoustical holography (NAH)", *J. Acoust. Soc. Am.* **107**, 3289-3297 (2000).

[7]. E. G. Williams, "Regularization methods for near–field acoustical holography", *J. Acoust. Soc. Am.* **110**, 1976-1988 (2001).

[8]. Y. Kim, P. A. Nelson, "Optimal regularization for acoustic source reconstruction by inverse methods", *J. Sound Vib.* **275**, 463-487 (2004).

[9]. A. N. Thite, D. J. Thompson, "Selection of response measurement locations to improve inverse force determination," *Applied Acoustics* **67**, 797–818 (2006).